Optical Materials 88 (2019) 586–593

Contents lists available at ScienceDirect

Optical Materials

journal homepage: www.elsevier.com/locate/optmat

Improved femtosecond third-order nonlinear optical properties of thin layered $Cu_3Nb_2O_8$

Priyadarshani N.[a], Sabari Girisun T.C.[a,*], Venugopal Rao S.[b]

[a] Nanophotonics Laboratory, School of Physics, Bharathidasan University, Tiruchirappalli, 620024, India
[b] Advanced Centre of Research in High Energy Materials (ACRHEM), University of Hyderabad, Hyderabad, 500046, Telangana, India

ARTICLE INFO

Keywords:
Copper niobate
Optical limiting
Femtosecond
Z-scan

ABSTRACT

Thin motif-layered triclinic $Cu_3Nb_2O_8$ was prepared through solid-state reaction at 700 °C, 12 h and their nonlinear optical (NLO) properties with ultrafast [800 nm, 150 fs (fs) pulses, 80 MHz repetition rate] pulse laser excitation were studied. A peculiar shift from reverse saturable absorption (RSA) to saturable absorption (SA) at a peak intensity of 40 MW/cm^2 was observed. The involvement of excited state absorption (ESA) is confirmed from the decrease in the nonlinear absorption coefficient with increase in peak intensity and the observed nonlinearity is ascribed to a sequential 2 PA process (1 PA + ESA). Formation of layered structure in $Cu_3Nb_2O_8$ acted as a transport layers which yielded high nonlinear absorption coefficient (7.8×10^{-10} m/W), nonlinear refractive index (5.17×10^{-16} m^2/W) and nonlinear optical susceptibility (25.6×10^{-11} esu) when compared to other known copper niobates. The observation of low onset-limiting threshold (78.79–26.26 μJ/cm^2) renders $Cu_3Nb_2O_8$ a prospective material for ultrashort pulse laser protecting device and biomedical microsurgery tools. A transition of mixed phase $CuNb_2O_6$–$Cu_3Nb_2O_8$ into pure triclinic $Cu_3Nb_2O_8$ along with change in morphology from pore to layered structure with increase in sintering time was confirmed from powder XRD, Raman, FESEM measurements and UV–Visible absorption studies.

1. Introduction

Ultrashort pulsed lasers find a special place in the world of optics with significant applications in the field of nonlinear optics, fiber-optic communications, material processing and, therefore, it is essential to investigate the femtosecond (fs) laser interaction with different materials and the corresponding third-order nonlinear optical (NLO) properties of the material [1]. Challenges in fulfilling the material's properties such as large nonlinear response, short response time and high damage threshold are the practical difficulties in the development of nonlinear optical devices suitable for ultrashort pulse lasers [2]. Since the laser technology had bloomed quick as a wink, protecting devices from the laser induced damages are believed to be promising need for the human as well as scientific community [3]. To the knowledge, optical limiting studies on the ultrashort pulse IR optical region lasers were very rarely investigated and reported. Organic dyes, conjugated systems like fullerene [4], porphyrin [5], phthalocyanine [6] and organometallic compounds [7] are some of the known optical limiting materials that are investigated in the femtosecond regime. Though these bench mark materials offer strong NLO behaviour, properties like poor transparency and stability against high power femtosecond lasers restrict the usage of these materials in the practical applications. To address the problems prevailed in the organic system, two dimensional layered materials are investigated because of its rich variety in terms of composition, structure, high diversity that offers tunable electrical and optical properties [8]. In the layered materials, though graphene family [9], single and multi-walled carbon tubes [10,11] provides better nonlinearity, a major issue of intrinsic energy band gap property motivated the researcher to explore other layered materials with semiconducting nature. Metal dichalcogenides, silicon, hexagonal boron nitride, phosphorene and metal oxides materials are under lime light of 2D layered materials as they possess thinnest isolated form without surface dangling bonds and outstanding transport intralayer [12]. In particular two dimensional metal oxide sheets offers high surface area and favourable electron transfer characteristics which is favourable for opto-electronic applications [13–16].

Among the metal oxide nanosheets, ternary niobium oxide system with a series of nanosheets and varied structures are very important because of their functional building blocks useful for various applications [17]. Incorporation of metal (copper oxide) into the niobium sheets overcomes the long term limitation of identifying wide band gap semiconductors with high optical nonlinearities and high laser damage

* Corresponding author.
E-mail addresses: sabarigirisun@bdu.ac.in (T.C. Sabari Girisun), soma_venu@uohyd.ac.in (S. Venugopal Rao).

https://doi.org/10.1016/j.optmat.2018.12.034
Received 8 September 2018; Received in revised form 18 December 2018; Accepted 19 December 2018
0925-3467/

threshold [18]. This complex system offers fast electron transport property, and improved nonlinear optical properties [19] by phonon drag effect where the photons emitted due to electron scattering in one layer gets absorbed in another layer. Numerous copper-niobium-oxygen complex systems can be obtained by varying the elemental composition and are generally classified into two types based on the monovalent and divalent nature of the copper atoms. Here triclinic $Cu_3Nb_2O_8$ falls under the divalent category in which Cu^{2+} ions in the system owns partially filled (d^9) orbitals. The major difference between the crystal structure of $CuNb_2O_6$ and $Cu_3Nb_2O_8$ is that $CuNb_2O_6$ consist of Cu—O_6 and Nb—O_6 octahedra that forms a chain like structure linked to share their edges and corners with the neighbouring edges and corners, while $Cu_3Nb_2O_8$ consists of Cu_3O_8 units which consist of two non-equivalent Cu atoms. Each Cu_3O_8 units combined to form the jagged copper-oxygen chains continued to form as a Cu—O layers, where Nb atoms piled up between the layers surrounded by six oxygen atoms octahedrally. The change in this crystal arrangement between the parental and the modified system is expected to bring a change in the band structure and recently superior corrosion resistance of $Cu_3Nb_2O_8$ is reported [20]. Our previous investigations on various phases of copper niobate (M-$CuNb_2O_6$, O—$CuNb_2O_6$, M-O—$CuNb_2O_6$ and M-$CuNbO_3$) demonstrated superior NLO properties because of the optical and thermal stability in the femtosecond regime compared to the benchmark materials like CNT, GO [21–23]. All these facts ignited the idea to extend the study of ultrashort pulse optical limiting behaviour of another copper-niobium-oxygen systems i.e., $Cu_3Nb_2O_8$. So this article reports the preparation of layered triclinic phase of $Cu_3Nb_2O_8$ and third order NLO properties studied in the femtosecond regime using Z-scan experiments.

2. Preparation and measurements

In the present work, attempts were made to prepare a layered $Cu_3Nb_2O_8$ and study their structural, morphological, linear optical and ultrafast (femtosecond laser excitation) third-order NLO properties. In solid state reaction, composition and sintering temperature are the major parameter that should be taken into account in attaining the desired phase composition. Earlier works on preparation of copper niobate with different phases like M-$CuNb_2O_6$,O—$CuNb_2O_6$, M-$CuNbO_3$and $CuNb_3O_8$ [21–23] showcase that sintering temperature and time influence the phase and morphology of copper niobate which in turn persuades its third-order nonlinear optical properties. So employing similar synthesis procedure, solid state reaction with various reaction time was adopted in the preparation of $Cu_3Nb_2O_8$. The stochiometric mixtures of the precursors Nb_2O_5 (Sigma Aldrich) and CuO (Merck) were taken in the molar ratio of 1:3 and well grounded using mortar. Wahlstrom et al., investigated the phase analysis in copper-niobium-oxygen systems and reported that triclinic $Cu_3Nb_2O_8$ can be obtained at sintering temperature of 700 °C [24]. Investigation on other compositon of copper niobate exposed the possible formation of parent compound $CuNb_2O_6$ at low sintering time [21]. So to provide adequate energy to transform and attain the desire phase from the parent structure the grounded samples were sintered at 700 °C for various sintering time of 3–12 h. XRD measurements were done to confirm the phase formation of the material using PAN analytical X-Ray powder diffractometer. As prolonged sintering alters the morphology, the prepared samples were subjected to FESEM studies using FEI Quanta FEG 200 scanning electron microscope. Linear optical properties were studied using Lamda UV–Vis spectrophotometer (200–1000 nm) and emission studies (excitation at 443 nm) by FP-8000 spectrofluorometer. The samples dispersed in diethylene glycol with linear transmittance of ~70% were used to study the third-order nonlinear optical properties. Nonlinear absorption and nonlinear refraction properties of the sample were retrieved by Z-scan experiment using Ti: Sapphire laser (800 nm, 150 fs, 80 MHz) as excitation source. The sample was made to move along the Z-direction of the focused beam and the light intensity were measured with the detector. Here the laser was focused through 100 mm convex lens with beam waist (ω_o) of ~25 μm corresponding to Rayleigh range of 2.54 mm. Using the experimental setup reported elsewhere [25], intensity dependent nonlinear absorption and optical limiting studies were performed at peak intensity of ~12–40 MW/cm^2.

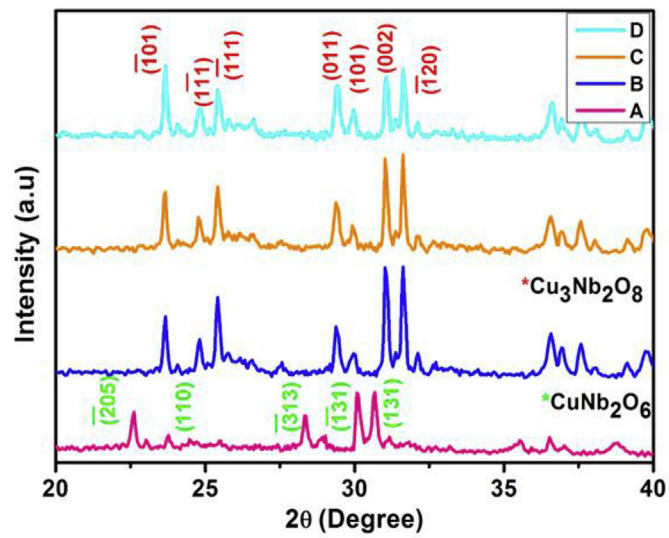

Fig. 1. XRD spectrum of $Cu_3Nb_2O_8$ sintered at 700 °C for (A) 3 h (B) 6 h (C) 9 h and (D) 12 h.

3. Results and discussion

3.1. Crystalline phase and morphology

XRD data of the samples investigated in this study is shown in Fig. 1 is used for preliminary identification and phase confirmation of synthesized samples. Materials sintered at 3 h were primely composed of $CuNb_2O_6$ along with minor traces of $Cu_3Nb_2O_8$ which was confirmed from the indexed peaks using JCPDS card no: 00-033-0476 and 01-086-034, respectively. At lower sintering time, the dominance of characteristic peaks of ($\bar{1}$31) and (131) of $CuNb_2O_6$ was evident and attributed to the major presence of parental crystal structure of copper niobate and the minimal traces of $Cu_3Nb_2O_8$ were due to chosen sintering temperature and starting precursor. A very similar kind of material formation was encountered in the preparaton of $CuNb_2O_6$ [21] and this is because the sintering time is insufficient to produce the desired phase structure of $Cu_3Nb_2O_8$. Increase in sintering time leads to a minor shift in the ($\bar{1}$31) and (131) peak indicating the formation of triclinic $Cu_3Nb_2O_8$ at 6 h of sintering with appearance of (002) and ($\bar{1}$20) [26]. Samples remain at triclinic crystal of $Cu_3Nb_2O_8$ at higher sintering time and the observed peak broadening emphasis the particle size reduction. $Cu_3Nb_2O_8$ is a centrosymmetric system that crystallizes in the P$\bar{1}$ space group with triclinic phase. As discussed earlier, the crystal structural arrangement of $CuNb_2O_6$ and $Cu_3Nb_2O_8$ differes in the sense that the building block Cu—O_6 are linked as chain in the former and Cu_3O_8 units combined as jagged chains in the latter [27]. The variation in the crystal structure was encountered from the shift in the vibrational bands of Raman spectra presented in Fig. 2. Broad vibration peaks around 260 cm^{-1}, 330 cm^{-1} and 360 cm^{-1} and narrow vibration in the region of 980 cm^{-1} and 1000 cm^{-1} were observed n both M-$CuNb_2O_6$ and T-$Cu_3Nb_2O_8$. The copper niobate shares their edges and corners of Nb—O in three possible ways and thus a three pairs of Nb—O_6 vibrations are observed. The peak around 260 cm^{-1} attributes to Cu—O_6 and Cu_3O_8 chain vibration and the assignment peak around 330 cm^{-1}, 980 cm^{-1} and 1000 cm^{-1} provides the information on the symmetric stretching vibration of the chain, bridging and terminal oxygen vibrations [28]. From Raman spectra it can be

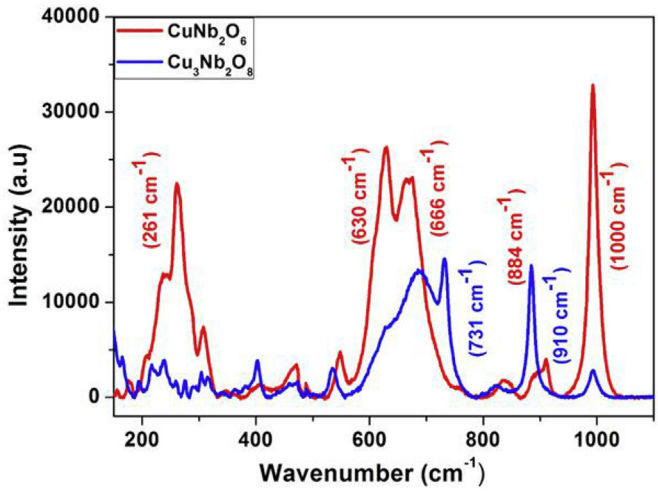

Fig. 2. Raman spectrum of parental structure monoclinic $CuNb_2O_6$ and derived structure triclinic $Cu_3Nb_2O_8$.

observed that terminal niobium oxygen (Nb−O_6) octahedra dominateswhich is witnessed through the raise in intensity of 1000 cm^{-1}. in pure $Cu_3Nb_2O_8$ compared to mixed phase prepared at 3 h. The minor shift in the Raman vibrations arises because $Cu_3Nb_2O_8$ consists of Cu_3O_8 chains with two non-equivalent copper atomswhile $CuNb_2O_6$contains Cu−O_6 and Nb−O_6 octahedral units. The morphotypes of the $Cu_3Nb_2O_8$ sintered at different time suffers a change and the growth mechanism of sample was studied by FESEM analysis. Initial sintering leads to local bonding to form a pore structure because of densification and mass transport and it resembles the textural arrangement of $CuNb_2O_6$ [29]. Increasing the sintering time to 6 h creates a continuous network with agglomorated layered structure, as the samples turn purely $CuNb_3O_8$.As the sintering time is further increased to 9 h, the layered networks appeared to be well-defined and shrinked. It is well known that during sintering process the layers gets shrinks depending on the sintering temperature and time. As the diffusion process continues because of the local heating effect (sintering) a considerable change in the thickness of the layers was encountered and a similar growth pattern was observed in CuO/Co_3O_4 layer [30]. At 12 h sintering a thin sheet like layer decomposes into hollow motif like pattern with abundant mesopores formed as alayer as shown in Fig. 3 (A-D) [30]. This kind of layered structure acts as a transport layers that improves the nonlinear absorption as well as refraction properties. The diagramatic representation below the recorded FESEM in Fig. 3 (E-H) shows the pictorial representation of the formation of hollow motif layered structure from inhomogenous agglomorated structure.

3.2. Ground-state absorption and emission

Linear absorption spectrum of the prepared samples was taken after dispersing the material in diethylene glycol and is shown in Fig. 4a. Thin motif layered $Cu_3Nb_2O_8$ (12 h) shows a broad absorption throughout UV–Vis region with absorption maxima at 297 nm corresponding to the energy of 4.1 eV. Fig. 4b represents the Tauc's plot drawn out from the absorption edge of linear spectrum and the band gap of T-$Cu_3Nb_2O_8$ was estimated to be 2.8 eV [21]. The FL spectrum of $Cu_3Nb_2O_8$with motif thin layers recorded at excitation wavelength of 443 nm is represented in Fig. 4c. $Cu_3Nb_2O_8$ shows a sharp blue emission (462 nm) and red emission (693 nm) which arises due to the charge transfer between the oxygen and niobium atoms (Nb−O). The proposed emission is because of the trapping of the excitons and niobium in the octahedra acts as luminescent centres due to the extrinsic niobates respectively. Sample sintered at 3 h resembles the UV–Visible absorption and FL emission pattern of $CuNb_2O_6$ with estimated band gap of 4.1 eV. Slight increase in bandgap compared to prevailing reported $CuNb_2O_6$ (3.5 eV) arises due to the minor traces of $Cu_3Nb_2O_8$ [31]. Here it is to be mentioned that $Cu_3Nb_2O_8$ with different morphotypes shows almost a similar linear optical properties.

3.3. Intensity dependent nonlinear absorption

Intensity dependent nonlinear absorption properties of the materials were studied by keeping the aperture open in front of the detector of Z-scan experiment. When performing Z-scan experiment on sample in the solution, it is important to note the effect of solvent. Therefore an open aperture pattern was recorded for diethylene glycol, to find whether the nonlinear absorption is purely because of copper niobate. Here the solvent does not show any nonlinear pattern which confirms the dispersing agent contribution was almost null. Fig. 5 shows the open aperture pattern of the samples excited with peak intensities in the 12–40 MW/cm^2 range. All the samples exhibited nonlinear absorption and the observed valley like pattern represent the presence of reverse saturable absorption (RSA) for all peak intensities. Peculiarly when excited at input peak power intensity of 40 MW/cm^2, the sample demonstrated saturable absorption (SA) which resulted in a transmittance increase (i.e. peak-like pattern was observed). Similar kind of switch over from RSA to SA pattern due to different dosage of electron beam irradiation was observed on Cu and Al doped ZnO thin films [13–16]. SA absorption is a one-photon nonlinear process and is induced by population bleaching of the ground state owing to an excited population that cannot relax to the ground state sufficiently fast at a large pump rate. In the recorded OA pattern (12–40 MW/cm^2), as the sintering time increases, strength of RSA also monotonically increases which is evidenced from deepening of valley pattern and for the layered structure of $Cu_3Nb_2O_8$ (sintered at 12 h) nonlinear absorption ascertain a maximum value. Here the origin of reverse saturable absorption or photodarkening effect may arise due to the following reason, i) the absorption at the exited state is higher than the ground state and ii) the molecules in the excited state can absorb the energy of the incident photon. To check the reliability of data and interpret the open aperture experimental value, a theoretical fit involving Sheik-Bahae [32] formalism for finding the involved mechanism was made. If α_n represents the multi-photon absorption coefficient (n = 2, 3), L is sample thickness, I_o is incident intensity at the focus, Z indicating the position of the sample and $Z_0 = \pi\omega_o^2/\lambda$ be the Rayleigh length [33], then normalized transmittance associated with nPA is,

$$T_{nPA} = \frac{1}{\left[1 + (n-1)a_n L \left(\frac{I_o}{1+\left(\frac{z}{z_o}\right)^2}\right)^{n-1}\right]^{\frac{1}{n-1}}}$$

RSA behaviour of the material arises due to any one of the nonlinear mechanisms such as 2 PA, 3 PA, excited state absorption, free carrier absorption or any combination of these process. Based on the above-mentioned equation the obtained pattern was theoretically fitted for both two and three photon mechanism and for the present case the theoretical equation of 2 PA fits well to the experimental data for all samples irrespective of peak-intensities. Generally, NLA occurs due to i) genuine multiphoton absorption process (nPA) – simultaneous absorption or ii) excited state absorption-sequential absorption and Z-scan technique cannot differentiate the mechanism involved in the nonlinear absorption process. For the occurrence of genuine 2 PA under the excitation of the IR laser (800 nm, 1.55 eV), the material must not have any energy state close to the excitation and possess a state around $2h\nu \geq E_g$. Here, from the band structure estimation of the material from UV–Vis absorption, it can be clearly witnessed that the material does not fulfil the requirement of genuine 2 PA. While two photon absorption is the most apparent process in the present case, the other possibility is that the excited electron absorbs two photon absorbs

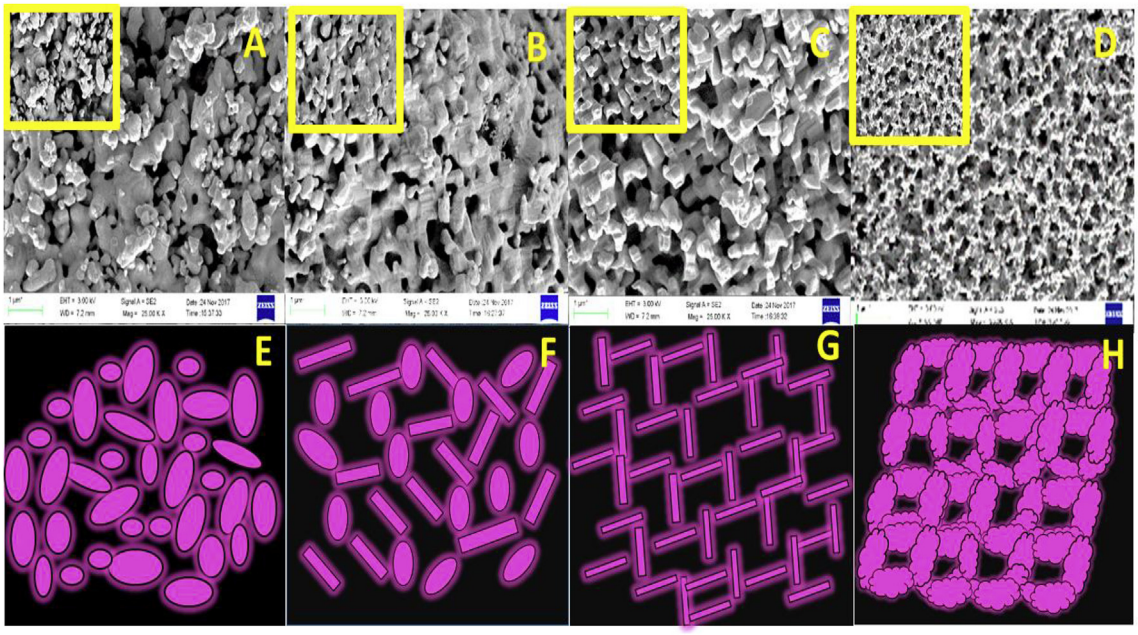

Fig. 3. A–D: FESEM analysis of $Cu_3Nb_2O_8$ sintered at different sintering time (3–12 h) at 700 °C. (E–H): The pictorial representation of transition from agglomorated structure to thin layered hollow motif structure of $Cu_3Nb_2O_8$ with increase in sintering time from 3 to 12 h.

sequentially through the defects states 693 nm (1.79 eV) to the band edge 443 nm (2.8 eV). Thus, it can be inferred that the observed nonlinear absorption may be a sequential 2 PA, and the possible involved transition is that the electron from the ground state transit to the available defect state (693 nm, 1.79 eV) through one photon absorption with the additional aid of non-radiative heat energy and sequentially absorbs one more photon from the defect state to reach the excited band edge state (443 nm, 2.8 eV) accompanied by the emission of excess energy in non-radiative form. The mechanism involved in nonlinear absorption can be further confirmed by measuring the intensity dependent nonlinear absorption coefficient. Plot of nonlinear absorption coefficient as a function of input intensity when remains consistent corresponds to genuine 2 PA and when changes, it refers to excited state absorption (ESA). At higher input peak intensity there will be an involvement of large number of photons involved in production of free carriers in the copper niobate crystal structure and that leads to strong one photon absorption brings up saturable absorption behaviour. From the intensity dependent absorption graph (Fig. 6), it can be inferred that nonlinear absorption co-efficient decreases with an increase in input intensity suggesting the contribution from 2 PA = 1 PA + ESA process. Hence, it can be comprehended from the ground-state absorption, numerical analysis, intensity-dependent nonlinear absorption studies that the perceived nonlinearity may emerges due to 1 PA + ESA. The estimated nonlinear absorption coefficient (Table 1) for layered $Cu_3Nb_2O_8$ (sintering at 12 h) was found to be higher than the known NLO systems like BBO (2.1×10^{-10} m/W) [34], Fe_2O_3 (0.82×10^{-12} m/W) [35], lead iodide perovskite (0.22×10^{-10} m/W) [36], ZnSe/PVA (2.6×10^{-10} m/W) [25], CdO (7.1×10^{-10} m/W) [37]. Also among the copper niobates investigated under similar condition, 2 PA coefficient of $Cu_3Nb_2O_8$was found to be higher than other derived phases of $CuNb_2O_6$ like mixed (monoclinic-orthorhombic) $CuNb_2O_6$ (-5.5×10^{-12} m/W), monoclinic-$CuNbO_3$ (2×10^{-12} m/W) which emphasizes the superiority of $Cu_3Nb_2O_8$ for femtosecond laser investigations.

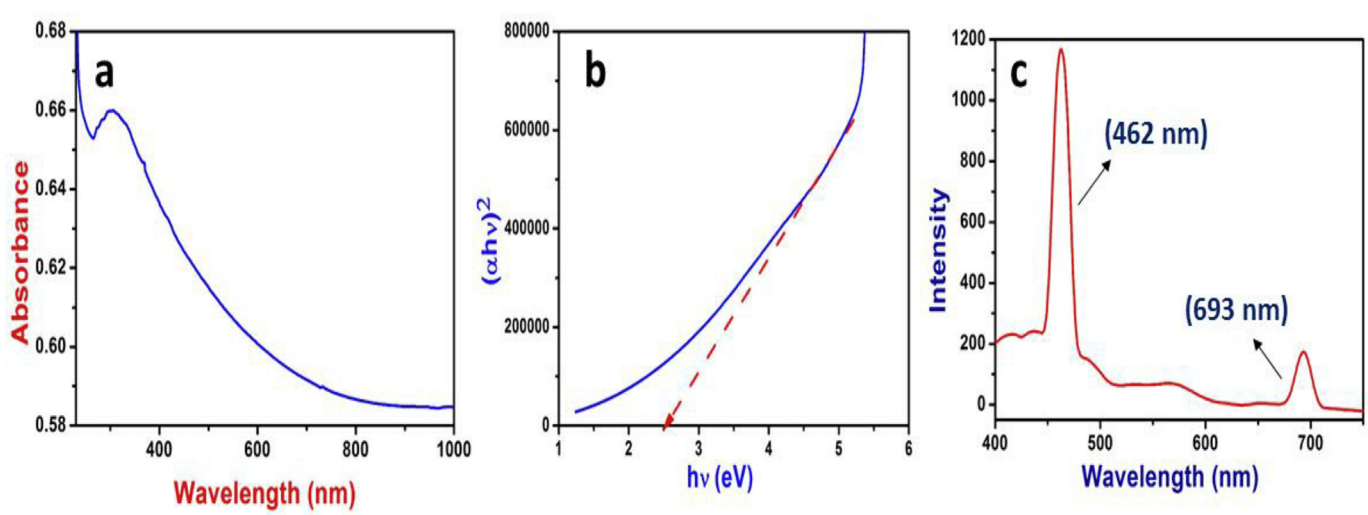

Fig. 4. (a) Linear absorption (b) Tauc's plot and (b) Emission spectrum of $Cu_3Nb_2O_8$ (sintered at 12 h).

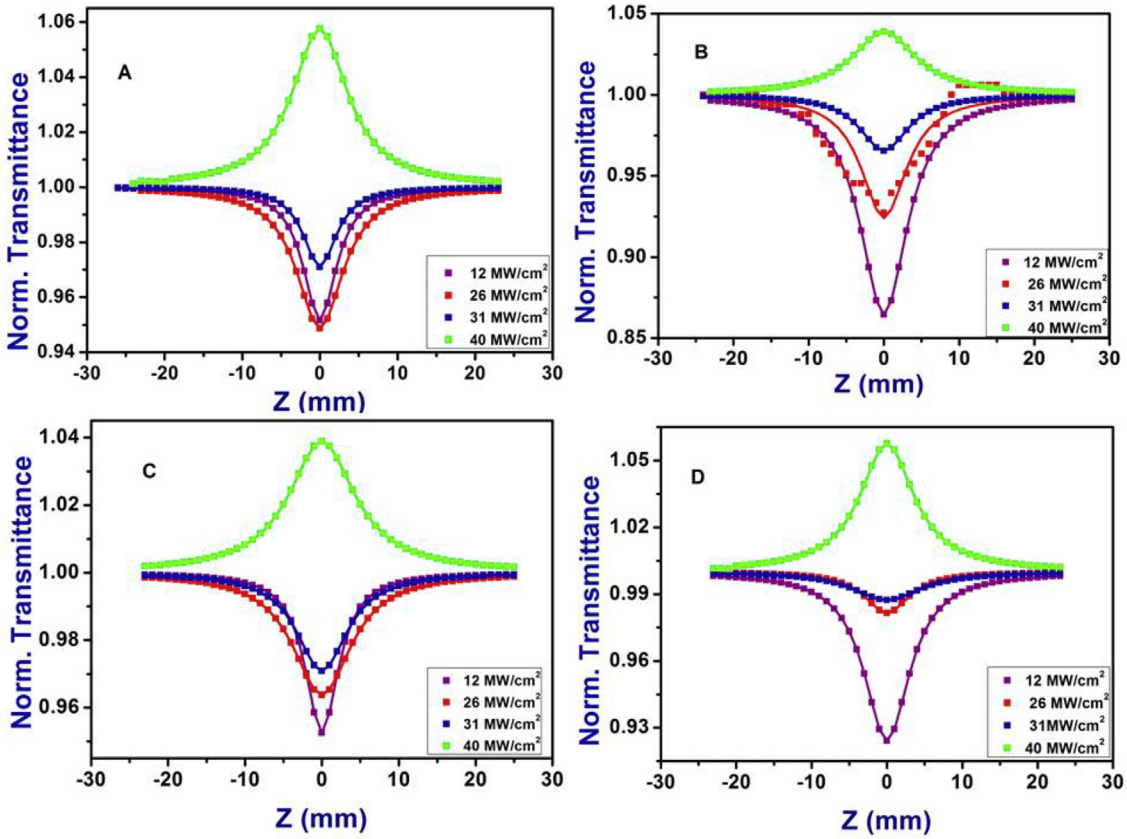

Fig. 5. Intensity dependent open aperture Z-scan data of $Cu_3Nb_2O_8$ sintered at (A) 3 h (B) 6 h (C) 9 h and (D) 12 h. Symbols represents the experimental data points and the solid lines are the theoritical fits drawn to the experimental data.

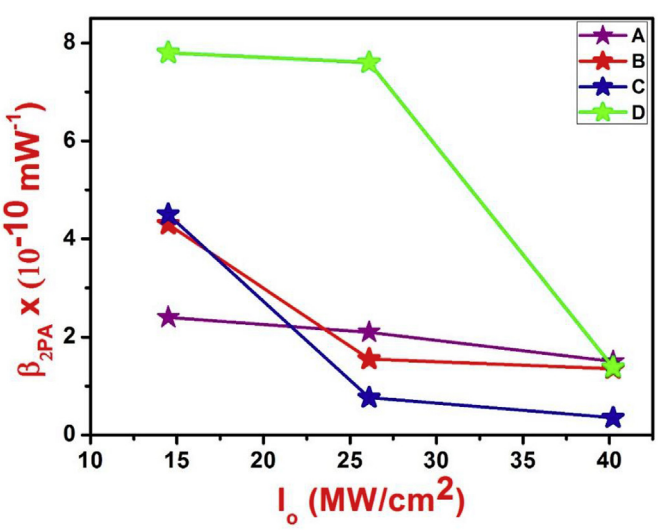

Fig. 6. The variation in nonlinear absorption co-efficient (β_{2PA}) as a function of peak power intensity of $Cu_3Nb_2O_8$ sintered at (A) 3 h (B) 6 h (C) 9 h and (D) 12 h.

Table 1
Summary of the third-order NLO parameters of $Cu_3Nb_2O_8$.

Third-order NLO parameters	A - 3 h	B - 3 h	C– 9 h	D- 12 h
Nonlinear absorption coefficient, ($\beta \times 10^{-10}$ m/W)				
12 MW/cm^2	−2.4	−4.3	−4.5	−7.8
26 MW/cm^2	−2.1	−1.55	−0.76	−7.6
31 MW/cm^2	−1.5	−1.35	−0.35	−1.38
40 MW/cm^2	+0.018	+0.012	+000.6	+0.002
Nonlinear refractive index (3 mW) ($n_2 \times 10^{-16}$ m^2/W)	1.21	1.49	2.45	5.17
Real susceptibility [Re (χ^3) $\times 10^{-11}$ esu]	5.99	8.16	12.13	25.59
Imaginary susceptibility [Im (χ^3) $\times 10^{-11}$ esu]	0.76	1.36	2.46	1.42
Third-order NLO susceptibility ($\chi^3 \times 10^{-11}$ esu)	5.99	7.35	12.13	25.6
Onset of Optical Limiting (μJ/cm^2)	78.79	60.32	47.49	26.26

3.4. Nonlinear refraction and optical limiting

Nonlinear refraction of $Cu_3Nb_2O_8$ was studied by performing closed aperture Z-scan experiment by keeping the aperture of detector almost closed. To avoid scattering issues, nonlinear refraction studies were performed only at low power (~12 MW/cm^2) which in turn highly influence the nonlinear refraction properties. In general, nonlinear refraction may arise due to thermal effect, molecular reorientation, excited state refraction, electronic polarization etc. Fig. 7b indicates the nonlinear closed aperture pattern of $Cu_3Nb_2O_8$. It is apparent that on excitation with the high repetition rate (80 MHz) fs laser, the nonlinear refraction of material is expected to be mainly thermal in origin. The presence of peak-valley pattern for all samples clearly depicts that $Cu_3Nb_2O_8$exhibit self-defocusing type nonlinear refraction. The experimental data was fitted theoretically using the equation [38].

$$T_{CA} = \pm \frac{4\Delta\phi \frac{z}{z_0}}{\left[1 + \left(\frac{z}{z_0}\right)^2\right]\left[9 + \left(\frac{z}{z_0}\right)^2\right]}$$

where z is the distance moved from the focus ($z = 0$) by the sample, z_0 is the Rayleigh range and $\Delta\phi$ is the phase change of the laser beam due to refraction. In the pattern, circles indicate the experimental data and

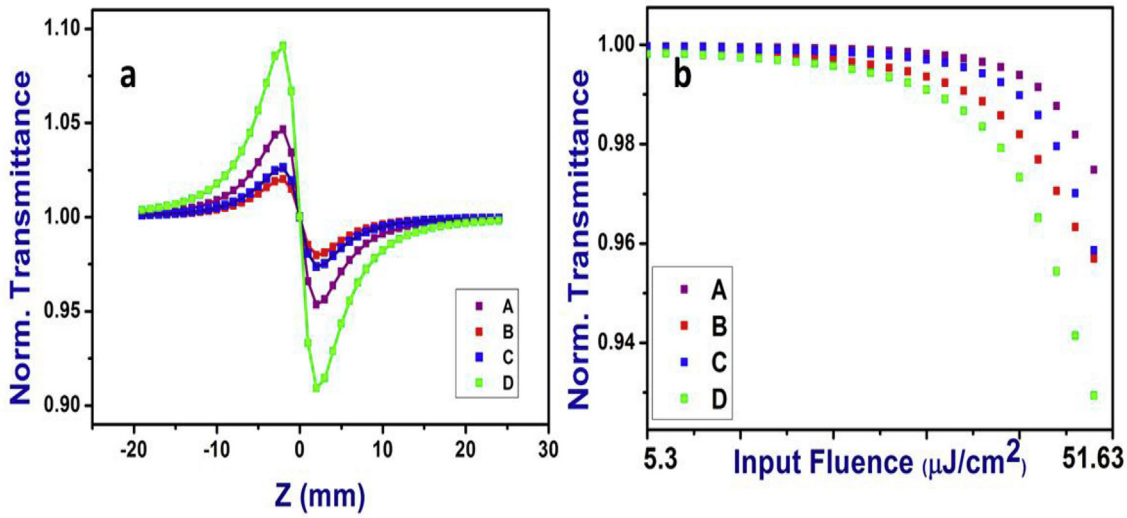

Fig. 7. (a) Closed aperture and (b) Optical limiting pattern of $Cu_3Nb_2O_8$ sintered at (a) 3 h (b) 6 h (c) 9 h and (D)12 h. Solid lines are the theoritical fits and the symbols are experimental points.

the solid lines to the theoretical fit. The magnitude of the nonlinear refractive index of the material was retrieved using Δϕ-phase from the relation, $n_2 = \Delta\phi/2\pi L_{eff} I_0$ and the estimated nonlinear refractive index were provided in Table 1. The closed aperture pattern shows that material acts like a thermal lens, initially converging the beam before the focus point (pre-focal peak) and then diverges away from focus (post-focal valley). Generally the negative refractive index was inhibited by thermal contribution and addition to that these heat conducting nonlocal behaviour were put to use in investigation of the nonlocal nonlinear phenomena. The heat transfer through the medium with a change in density of the medium leads to variation in the refractive index. As expected nonlinear refractive index were higher for the thin layered $Cu_3Nb_2O_8$ than the microstructures. The interlayer interaction within the material play an important role in the nonlinear optical properties. The nonlinear refractive index value was found to be higher for the layered structure due to stacking [39]. Nonlinear refractive index values are found to be comparable with the well-known NLO systems likelithium borate (0.26×10^{-17} m^2/W) [40], Fe_2O_3 (4.94×10^{-20} m^2/W) [41], graphene oxide (3×10^{-14} m/W) [42], CuO and Cu_2O (3.96×10^{-17} m^2/W and 2.81×10^{-17} m^2/W) [43].

IR optical limiting response of $Cu_3Nb_2O_8$ using Ti:sapphire laser at 800 nm were investigated. To escape from the scattering issues low concentration were taken to study the resultant limiting action and were displayed in Fig. 7b. From the open aperture pattern, optical limiting pattern were extracted and drawn between the normalized transmittance and the input fluence extracted with the aid of the relation [44]$F(z) = 4\sqrt{In2}\left(\frac{E_{in}}{\pi^{3/2}.\omega(z)^2}\right)$, the input fluence was calculated with respect to the position of the sample and E_{in} is the input energy of the laser. At low input incidence, the normalized transmittance obeys Beer-Lambert law and thus linearly increases with input power. The nonlinearity occurs at certain limit called as onset-limiting threshold and beyond which the transmittance of the samples deviate from linearity [45]. Typically, an optical limiting action occurs due to reverse saturable absorption or excited state absorption. An ideal optical limiter should possess low limiting threshold and in the present case the prepared sample shows limiting in the range of 78.79–26.26 μJ/cm^2 as given in Table A1. The limiting behaviour drastically decreased because of the layered oxide formation as encountered in the FESEM analysis. This is because, in two dimensional layered materials ultrafast nonlinear absorption will be higher compared to microstructure [46]. The limiting action was compared with the materials like Ag (1.7 J/cm^2) [47], fullerene (0.4 J/cm^2) [48], gold precipitated glass (0.03 J/cm^2) [49], duran glass (35 μJ/cm^2) [50] and the limiting threshold was low for $Cu_3Nb_2O_8$ as a layered structure and thus can be used as a competent material for high power optical limiting applications.

3.5. Third-order nonlinear optical coefficients

From the data presented in Table 1 it can be inferred that as sintering time increases the 2 PA coefficient was found to be increasing. At lower peak intensity 12 MW/cm^2, layered $Cu_3Nb_2O_8$ (12 h) possess the maximum 2 PA coefficient and is almost three times higher than pore structured mixed phase of $CuNb_2O_6$–$Cu_3Nb_2O_8$. The enhancement in the nonlinear absorption coefficient emphasizes the strong contribution from the layered morphotype and crystal phase arrangement of $Cu_3Nb_2O_8$. As peak intensity of excitation is increased, the nonlinear absorption coefficient decreases till 1.38×10^{-10} m/W and becomes positive (SA) at 40 MW/cm^2 Nonlinear refractive index also varies in a similar way as that of nonlinear absorption and layered $Cu_3Nb_2O_8$ possess the maximum value which is four times higher the samples sintered at lower sintering time (mixed phase). $\chi^{(3)}$, is a complex quantity that the material possesses its real and imaginary parts inherently. The former is related to the nonlinear refractive index, $n_2 \propto$ Re [$\chi^{(3)}$] and the latter to the two-photon absorption (2 PA) coefficient, $\beta \propto$ Im[$\chi^{(3)}$]. Using the below mentioned equation, the third order nonlinear optical susceptibility [51] can be obtained as,

$$Im\,[\chi^{(3)}] = 10^{-2}\frac{\varepsilon_0 n_0^2 c^2 \lambda}{4\pi^2}\beta\,(cm/W)\,,\; Re[\chi^{(3)}] = 10^{-4}\frac{\varepsilon_0 c^2 n_0^2}{\pi} n_2 (cm^2/W)$$

Real and imaginary part of the $\chi^{(3)}$ equally contributes in the optical nonlinearity of the material and the estimated values are given in Table 1. In the present case, the value of the real $\chi^{(3)}$ is higher than the imaginary $\chi^{(3)}$ which justifies the fact that nonlinear refractive effect dominates the nonlinearity. The nonlinear optical susceptibility was found to be one order higher for layered niobates which is due to the transformation of bulk material (1.21×10^{-11} esu) into nanolayers (25×10^{-11} esu). Large nonlinear susceptibility was observed in the present work compared to other favourable semiconductors like bismuth tellurite glass (4.73×10^{-14} esu) [52], Au:SiO_2 (10^{-12} esu) [53] and layered materials like GO-porphyrin (10^{-12} esu) [54], MoS_2 (10^{-15} esu) [55], CS_2 (10^{-14} esu) [56]. An error of almost 10% is expected in the obtained value represented in Table 1 due to various factors like estimation of input intensity and theoretical fit plotted to the experimental data. For comparison, third-order nonlinear optical coefficients of different phase of copper niobate along with other well-known NLO systems excited under under similar experimental

Table 2
Third-order NLO parameters of parental and derived copper niobate systems and other well-known NLO systems excited using femtosecond laser (800 nm, 150 fs, ~80 MHz).

Sample	Nonlinear absorption coefficient (m/W)	Nonlinear refractive index (m^2/W)	Third-order nonlinear optical susceptibility (esu)	Limiting threshold ($\mu J/cm^2$)	Reference
Monoclinic $CuNb_2O_6$	85×10^{-10}	4.13×10^{-12}	6.74×10^{-10}	0.26	[21]
Mixed (Monoclinic: Orthorhombic) $CuNb_2O_6$	0.4×10^{-12}	2.3×10^{-17}	1.2×10^{-11}	–	[22]
Monoclinic $CuNbO_3$	0.51×10^{-12}	3.1×10^{-17}	1.53×10^{-11}	47.49	[23]
Monoclinic $CuNb_3O_8$	5.4×10^{-10}	2.15×10^{-16}	1.4810^{-11}	34.60	–
Triclinic $Cu_3Nb_2O_8$	7.8×10^{-10}	5.17×10^{-16}	25.6×10^{-11}	26.26	[Present]
Zinc porphyrin	5.0×10^{-10}	0.5×10^{-16}	1.3×10^{-9}	37	[58]
Glucuronic acid γ Lactone	3.51×10^{-10}	7.2×10^{-17}	29.3×10^{-12}	–	[59]
Au -Ag Core - shell nanorods	$0.5–2.0 \times 10^{-10}$	$0.2–0.8 \times 10^{-18}$	–	–	[60]
Ni(II), Cu(II) and Zn(II) complexes	$0.23–0.27 \times 10^{-9}$	$3.4–3.5 \times 10^{-20}$	–	–	[61]
BBO	2.1×10^{-10}	0.3×10^{-12}	1.3×10^{-10}	0.50	[34]

conditions (Ti: Sapphhire laser 800 nm, 150 fs, 80 MHz) is given in Table 2. It is interesting to be observed that NLO coefficients was found to be varying strongly with the crystal structural arrangement and its morphology. Thus it can be clearly witnessed that sintering temperature and time of solid-state reaction plays a predominant role in achieving stronger nonlinearity. Among the investigated phases of copper niobate, the parental structure ie., monoclinic $CuNb_2O_6$ possess stronger nonlinearity than its derived structure and other NLO systems.

And in the derived structure, $Cu_3Nb_2O_8$ possess higher nonlinear 2 PA coefficient, nonlinear refractive index and third-order NLO susceptibility due to the presence of motif layered morphology and modified crystal structure from the parent compound (inequivalent copper chains and the jagged Nb between the chains). Generally the niobium octahedral system itself possesses high nonlinearity because of its metal oxygen bond in the structural coordinates. The multiferroic magnetic nature of $Cu_3Nb_2O_8$ is also the reason behind the enhancement in nonlinear optical property of the sample making them to be a suitable material for the limiting applications. The position of the niobium due to the variation in the copper size will bring the distortion in the crystal structure of the material and this may possibly lead to the improvement in the susceptibility value [57]. The development of new $\chi^{(3)}$ materials is essential for the advancement of nonlinear optics, especially for applications that require high power and longer wavelengths throughout the infrared (IR) and $Cu_3Nb_2O_8$ with higher $\chi^{(3)}$ can be potential material for laser safety devices against ultrashort pulse IR lasers.

4. Conclusions

Two-dimensional $Cu_3Nb_2O_8$ layers were achieved by a simple solid-state reaction at 700 °C, 12 h. XRD and Raman showcase that prolonged sintering have made a transformation of parent monoclinic $CuNb_2O_6$ to triclinic $Cu_3Nb_2O_8$. Along with crystal structural phase transformation, the morphotype of $Cu_3Nb_2O_8$ transit themselves into hollow motif like pattern with abundant mesoporous at 12 h of sintering. T- $Cu_3Nb_2O_8$ exhibit reverse saturable absorption ascribed due to 2 PA process. Decrease in nonlinear absorption coefficient with increase in peak intensity ascertains the involved 2 PA process as 1 PA + ESA. Sequential absorption of two photons were confirmed through linear optical studies and the possible transition is $E_0 \rightarrow E_1$ (693 nm, 1.79 eV) $E_2 \rightarrow E3$ (443, 2.8 eV). At higher peak intensity 40 MW/cm^2, switching of nonlinear absorption pattern i.e., RSA to SA was observed due to the bleaching of ground state. Nonlinear refraction studies were carried out at low input intensity of 12 MW/cm^2 shows that all the samples exhibit self-focusing behaviour with maximum negative nonlinear refractive index for the layered structure (5.17×10^{-16} m^2/W). Observed ultrafast nonlinear refraction induces optical limiting action with onset limiting threshold of (78.79–26.26) $\mu J/cm^2$. Tunable third order NLO coefficients under femtosecond laser arises mainly due to the change in morphotype and better nonlinearity was observed for layered copper niobate due to high surface area and high electron transfer properties.

Declaration of interests

The authors declare that they have no known competing financial interests or personal relationships that could have appeared to influence the work reported in this paper.

Acknowledgments

Ms. N. Priyadarshani wishes to thank University Grants Commission, Government of India for providing UGC-SAP (RFMS) fellowship to carry out her research work (Grant No: F.25-1/2014-15 (BSR)/No.F.7-197/2007). S.V. Rao acknowledges the support from DRDO, India.

References

[1] S. Nolte, F. Schrempel, F. Dausinger, Ultrashort Pulse Laser Technology, vol. 1, Springer International Publishing, 2016.
[2] L. Li, S. Jiang, Y. Wang, X. Wang, L. Duan, D. Mao, Z. Li, B. Man, J. Si, WS_2/fluorine mica (FM) saturable absorbers for all-normal-dispersion mode-locked fiber laser, Optic Express 23 (2015) 28698–28706.
[3] B. Schwarz, G. Ritt, M. Koerber, B. Eberle, Laser-induced damage threshold of camera sensors and micro-optoelectromechanical systems, Opt. Eng. 56 (2017) 034108–034111.
[4] Z.B. Liu, J.G. Tian, W.P. Zang, W.Y. Zhou, C.P. Zhang, J.Y. Zheng, Y.C. Zhou, H. Xu, Large optical nonlinearities of new organophosphorus fullerene derivatives, Appl. Opt. 42 (2003) 7072–7076.
[5] M.O. Senge, M. Fazekas, E.G.A. Notaras, W.J. Blau, M. Zawadzka, O.B. Locos, E.M. Ni Mhuircheartaigh, Nonlinear optical properties of porphyrins, Adv. Mater. 19 (2007) 2737–2774.
[6] P.T. Anusha, A.R. Thomas, R. Philip, S. Venugopal Rao, Nonlinear absorption and excited state dynamics of porphyrin and phthalocyanine in the presence of explosive molecules, Chem. Phys. Lett. 641 (2015) 23–28.
[7] D. Swain, R. Singh, V.K. Singh, N.V. Krishna, L. Giribabu, S. Venugopal Rao, Sterically demanded zinc(II) phthalocyanines: synthesis, optical, electrochemical, nonlinear optical, excited state dynamics studies, J. Mater. Chem. C 2 (2014) 1711–1722.
[8] J. Szeremeta, R. Kolkowski, M. Nyk, M. Samoc, Wavelength dependence of the complex third-order nonlinear optical susceptibility of poly(3-hexylthiophene) studied by femtosecond Z-scan in solution and thin film, J. Phys. Chem. C 117 (2013) 26197–26203.
[9] G.R. Bhimanapati, Z. Lin, V. Meunier, Y. Jung, J. Cha, S. Das, D. Xiao, Y. Son, M.S. Strano, V.R. Cooper, L. Liang, S.G. Louie, E. Ringe, W. Zhou, S.S. Kim, R.R. Naik, B.G. Sumpter, H. Terrones, F. Xia, Y. Wang, J. Zhu, D. Akinwande, N. Alem, J.A. Schuller, R.E. Schaak, M. Terrones, J.A. Robinson, Recent advances in two-dimensional materials beyond graphene, ACS Nano 9 (2015) 11509–11539.
[10] D. Shimamoto, T. Sakurai, M. Itoh, Y.A. Kim, T. Hayashi, M. Endo, M. Terrones, Nonlinear optical absorption and reflection of single wall carbon nanotube thin films by Z-scan technique, Appl. Phys. Lett. 92 (1–3) (2008) 081902–081905.
[11] H.I. Elim, W. Ji, G.H. Ma, K.Y. Lim, C.H. Sow, C.H.A. Huan, Ultrafast absorptive and refractive nonlinearities in multiwalled carbon nanotube films, Appl. Phys. Lett. 85 (2004) 1799–1801.
[12] Z. Liu, S. Ping Lau, F. Yan, Functionalized graphene and other two-dimensional materials for photovoltaic devices: device design and processing, Chem. Soc. Rev.

44 (2015) 5638–5679.
[13] Albin Antony, P. Poornesh, I.V. Kityk, K. Ozga, Ganesh Sanjeev, Vikash Chandra Petwal, Vijay Pal Verma, Jishnu Dwivedi, A novel approach for tailoring structural, morphological, photoluminescence and nonlinear optical features in spray coated Cu:ZnO nanostructures *via* e-beam, CrystEngComm 20 (2018) 6502–6518.
[14] Albin Antony, P. Poornesh, I.V. Kityk, G. Myronchuk, Ganesh Sanjeev, Vikash Chandra Petwal, Vijay Pal Verma, Jishnu Dwivedi, A study of 8 MeV e-beam on localized defect states in ZnO nanostructures and its role on photoluminescence and third harmonic generation, J. Lumin. 207 (2019) 321–332.
[15] Albin Antony, S. Pramodini, P. Poornesh, I.V. Kityk, A.O. Fedorchuk, Ganesh Sanjeev, Influence of electron beam irradiation on nonlinear optical properties of Al doped ZnO thin films for optoelectronic device applications in the cw laser regime, Opt. Mater. 62 (2016) 64–71.
[16] Albin Antony, S. Pramodini, I.V. Kityk, M. Abd-Lefdil, A. Douayar, F. Cherkaoui El Moursli, Ganesh Sanjeev, K.B. Manjunatha, P. Poornesha, Effect of electron beam on structural, linear and nonlinear properties of nanostructured Fluorine doped ZnO thin films, Physica E 94 (2017) 190–195.
[17] K. Akatsuka, G. Takanashi, Y. Ebina, M. Haga, T. Sasaki, Electronic band structure of exfoliated titanium- and/or niobium-based oxide nanosheets probed by electrochemical and photoelectrochemical measurements, J. Phys. Chem. C 116 (2012) 12426–12433.
[18] I.B. Angelov, A.V. Conta, S.A. Trushina, Z. Major, S. Karsch, F. Krausza, V. Pervak, Investigation of the laser-induced damage in dispersive coatings, Proc. SPIE 8190 (2011) 81900B-1-5.
[19] P.J. Price, Two-dimensional electron transport in semiconductor layers. I. Phonon scattering, Ann. Phys. 133 (1981) 217–239.
[20] S. Kamimura, N. Murakami, T. Tsubota, T. Ohno, Fabrication and characterization of a p-type $Cu_3Nb_2O_8$ photocathode toward photoelectrochemical reduction of carbon dioxide, Appl. Catal., B 174 (2015) 471–476.
[21] N. Priyadarshani, S. Venugopal Rao, T.C. Sabari Girisun, Investigation of the femtosecond optical limiting properties of monoclinic copper niobate, Appl. Phys. B 122 (1–8) (2016) 256.
[22] N. Priyadarshani, T.C. Sabari Girisun, S. Venugopal Rao, Influence of sintering time on switching of the femtosecond nonlinear optical properties of $CuNb_2O_6$, Opt. Mater. 66 (2017) 534–541.
[23] N. Priyadarshani, T.C. Sabari Girisun, S. Venugopal Rao, Ultrafast nonlinear optical studies of equiaxed $CuNbO_3$ microstructures, Chem. Phys. Lett. 681 (2017) 95.
[24] E. Wahlstrom, B.O. Marinder, Phase analysis in copper-niobium-oxygen systems, Inorg. Nucl. Chem. Lett. 13 (1977) 559–564.
[25] M.C. Divyasree, E. Shiju, Jaismon Francis, P.T. Anusha, S. Venugopal Rao, K. Chandrasekharan, ZnSe/PVP nanocomposites: synthesis, structural and nonlinear optical analysis, Mater. Chem. Phys. 197 (2017) 208–214.
[26] G. Sharma, J. Saha, S.D. Kaushik, V. Siruguri, S. Patnaik, Improper ferroelectricity in helicoidal antiferromagnet Cu3Nb2O8, Solid State Commun. 203 (2015) 54–57.
[27] N. King, P.P. Sahoo, L. Fuoco, S. Stuart, D. Dougherty, Y. Liu, P.A. Maggard, Copper deficiency in the p-type semiconductor $Cu_{1-x}Nb_3O_8$, Chem. Mater. 26 (2014) 2095–2104.
[28] F. Huang, Q. Zhou, C. Ma, L. Li, X. Huang, F. Li, Q. Cui, D. Xu, W. Wang, T. Cui, G. Zou, High pressure Raman scattering and X-ray diffraction studies of $MgNb_2O_6$, RSC Adv. 3 (2013) 3210–13213.
[29] L. Gary Messing, J. Adam Stevenson, Material Science: toward pore-free ceramics, Mater. Sci. 322 (2008) 383–384.
[30] K. Wang, B. Lv, H. Wu, X. Luo, J. Xu, Z. Geng, Soft-template-synthesis of hollow CuO/Co3O4composites for pseudo-capacitive electrode: a synergetic effect on electrochemical performance, J. Solid State Chem. 244 (2016) 75–83.
[31] N. Priyadarshani, T.C. Sabari Girisun, C. Ravidhas, Enhanced electrical behaviour of monoclinic p-$CuNb_2O_6$, Mater. Res. Bull. 84 (2016) 39–45.
[32] M.S. Bahae, A.A. Said, T. Wei, D.J. Hagan, E.W.V. stryland, Sensitive measurement of optical nonlinearities using a single beam, IEEE J. Quant. Electron. 26 (1990) 60–769.
[33] D. Swain, P.T. Anusha, T.S. Prashant, S.P. Tewari, T. Sarma, P.K. Panda, S. Venugopal Rao, Ultrafast excited state dynamics and dispersion studies of nonlinear optical properties in dinaphthoporphycenes Appl, Phys. Lett. 100 (1–5) (2012) 141109.
[34] T.C. Sabari Girisun, R. Madhura Somayaji, N. Priyadarshani, S. Venugopal Rao, Femtosecond third order optical nonlinearity and optical limiting studies of (γ and β) -Barium borate nanostructures, Mater. Res. Bull. 87 (2017) 102–108.
[35] P. Thomas, P. Sreekanth, K.E. Abraham, Nanosecond and ultrafast optical power limiting in luminescent Fe_2O_3 hexagonal nanomorphotype, J. Appl. Phys. 117 (2015) 053103–053109.
[36] B.S. Kalanoor, L. Gouda, R. Gottesman, S. Tirosh, E. Haltzi, A. Zaban, Y.R. Tischler, Third-Order optical nonlinearities in organometallic methylammonium lead iodide perovskite thin films, ACS Photonics 3 (2016) 361–370.
[37] P. Thomas, P. Sreekanth, R. Philip, K.E. Abraham, Morphology dependent nanosecond and ultrafast optical power limiting of CdO nanomorphotypes, RSC Adv. 5 (2015) 35017–35025.
[38] G. Jagannath, B. Eraiah, K. Naga Krishnakanth, S. Venugopal Rao, Linear and nonlinear optical properties of gold nanoparticles doped borate glasses, J. Non-Cryst. Solids 482 (2018) 160–169.
[39] W. Chen, G. Wang, S. Qin, C. Wang, J. Fang, J. Qi, X. Zhang, L. Wang, H. Jia, S. Chang, The nonlinear optical properties of coupling and decoupling graphene layers, AIP Adv. 3 (2013) 042123–0421129.
[40] H.P. Li, C.H. Kam, Y.L. Lam, W. Ji, Femtosecond Z-scan measurements of nonlinear refraction in nonlinear optical crystals, Opt. Mater. 15 (2001) 237–242.
[41] S. Lin, J. Fang, Y. Huang, Y. Zhang, J. Zhong, W. Xiang, X. Liang, Study on the iron oxide/glass nanocomposite materials: fabrication, microstructure and ultrafast nonlinear optical properties, J. Mater. Sci. Mater. Electron. 28 (2017) 17735–17743.
[42] L. Ran, Z. Chai, Y. Gao, W. Wu, Q. Chang, D. Kong, The nonlinear absorption of graphene oxide water solution in femtosecond regime, Curr. Appl. Phys. 16 (2016) 985–988.
[43] G. Yang, A. Chen, M. Fu, H. Long, P. Lu, Excimer laser deposited CuO and Cu_2O films with third-order optical nonlinearities by femtosecond Z-scan measurement, Appl. Phys. A 104 (2011) 171–175.
[44] M. Saravanan, T.C. Sabari Girisun, G. Vinitha, S. Venugopal Rao, Improved third-order optical nonlinearity and optical limiting behaviour of (nanospindle and nanosphere) zinc ferrite decorated reduced graphene oxide under continuous and ultrafast laser excitation, RSC Adv. 6 (2016) 91083–91092.
[45] Y. Zhan, Z. Zhao, C. Ba Vao, L. Yang, J. Li, P. Yuan, The nonlinear absorption and optical limiting in phenoxy-phthalocyanines liquid in nano- and femto-second regime: experimental studies, Opt, Laser Technol. 58 (2014) 207–214.
[46] S. Lu, Y. Ge, Z. Sun, Z. Huang, R. Cao, C. Zhao, S. Wen, D. Fan, J. Li, H. Zhang, Ultrafast nonlinear absorption and nonlinear refraction in few-layer oxidized black phosphorus, Photon. Res. 6 (2016) 286–292.
[47] S. Porel, N. Venkatram, D. Narayana Rao, T.P. Radhakrishnan, Optical power limiting in the femtosecond regime by silver nanoparticle–embedded polymer film, J. Appl. Phys. 103 (1–6) (2007) 033107.
[48] N. Kamanina, S. Putilin, D.S. Ko, Nano-, pico- and femtosecond study of fullerene-doped polymer-dispersed liquid crystals: holographic recording and optical limiting effect, Synth. Met. 127 (2002) 129–133.
[49] S. Qu, Y. Gao, X. Jiang, H. Zeng, Y. Song, J. Qiu, C. Zhu, K. Hirao, Nonlinear absorption and optical limiting in gold-precipitated glasses induced by a femtosecond laser, Optic Commun. 224 (2003) 321–327.
[50] K. Jamshidi-Ghaleh, N. Mansour, Nonlinear absorption and optical limiting in Duran glass induced by 800 nm femtosecond laser pulses, J. Phys. D Appl. Phys. 40 (2007) 366–369.
[51] M. Saravanan, T.C. Sabari Girisun, S. Venugopal Rao, Super-paramagnetic and unusual nonlinear absorption switching behavior of an in situ decorated $CdFe_2O_4$–rGO nanocomposite, J. Mater. Chem. C. 5 (2017) 9929–9942.
[52] P. Yadav, A. Sharma, Study of third-order optical nonlinearities of Se-Sn (Bi,Te) quaternary chalcogenide thin films using Ti: sapphire laser in femtosecond regime, J. Electron. Mater. 46 (2017) 312–320.
[53] H.B. Liao, R.F. Xiao, J.S. Fu, H. Wang, K.S. Wong, G.K.L. Wong, Origin of third-order optical nonlinearity in Au:SiO_2 composite films on femtosecond and picosecond time scales, Opt. Lett. 23 (1998) 388–390.
[54] M.B.M. Krishna, V.P. Kumar, N. Venkatramaiah, R. Venkatesan, D. Narayana Rao, Nonlinear optical properties of covalently linked graphene-metal porphyrin composite materials, Appl. Phys. Lett. 98 (1–3) (2011) 081106.
[55] K. Wang, J. Wang, J. Fan, M. Lotya, A. O'Neill, D. Fox, Y. Feng, X. Zhang, B. Jiang, Q. Zhao, H. Zhang, J.N. Coleman, L. Zhang, W.J. Blau, Ultrafast saturable absorption of two-dimensional MoS_2 nanosheets, ACS Nano 7 (2013) 9260–9267.
[56] X.Q. Yan, X.L. Zhang, S. Shi, Z.B. Liu, J.G. Tian, Third-order nonlinear susceptibility tensor elements of CS_2 at femtosecond time scale, Optic Express 19 (2011) 5559–5564.
[57] R.D. Johnson, Sunil Nair, L.C. Chapon, A. Bombardi, D. Prabhakaran, C. Vecchini, A.T. Boothroyd, P.G. Radaelli, $Cu_3Nb_2O_8$: a multiferroic with chiral coupling to the crystal structure, Phys. Rev. Lett. 107 (2011) 137205.
[58] M.S.S. Bharathi, S. Bhattacharya, J.V. Suman Krishna, L. Giribabu, S. Venugopal Rao, Femtosecond, broadband nonlinear optical studies of zinc porphyrin and zinc phthalocyanine, Optic Laser. Technol. 108 (2018) 418–425.
[59] R.K. Saripalli, K. Naga Krishnakant, S. Venugopal Rao, H.L. Bhat, Suja Elizabeth, Non-critically phase-matched second harmonic generation and third order nonlinearity in organic crystal glucuronic acid γ-lactone, J. Appl. Phys. 122 (2017) 223110.
[60] X.L. Liu, F. Nan, Y.H. Qiu, D.J. Yang, S.J. Ding, Q.Q. Wang, Large third-order optical susceptibility with good nonlinear figures of merit induced by octupole plasmon resonance of asymmetric Au-Ag core-shell nanorods, J. Phys. Chem. 122 (2018) 2958–3964.
[61] H. Liu, L. Wu, F. Li, X. Wang, H. Pan, Y. Ni, J. Yang, S. Li, Y. Tian, J. Wu, Syntheses, characterizations and third-order NLO properties of a series of Ni(II), Cu(II) and Zn (II) complexes using a novel S-benzyldithiocarbazate ligand, Polyhedron 121 (2017) 53–60.